$Cu^{63}(\gamma,n)Cu^{62}$ cross-section curve.[7-11] Sagane has shown that the yield ratio, $Mo^{92}(\gamma,n)Mo^{91}/Mo^{92}(\gamma,n)Mo^{91m}$, remains constant from about 15 Mev to 67 Mev.[12] Perlman and Friedlander[13] measured relative yields of sixteen (γ,n) reactions at 50 Mev and 100 Mev, and found that results at both energies agreed within experimental error.

In view of these facts, it seems doubtful that the yield ratio for the Br^{80} isomers should significantly

[7] B. C. Diven and D. M. Almy, Phys. Rev. 80, 407 (1950).
[8] L. L. Newkirk, Phys. Rev. 86, 2491 (1952).
[9] L. Katz and A. G. W. Cameron, Can. J. Phys. 29, 518 (1951).
[10] R. Sagane, Phys. Rev. 83, 174 (1951).
[11] A. I. Berman and K. L. Brown, Phys. Rev. 96, 83 (1954).
[12] R. Sagane, Phys. Rev. 85, 926 (1952).
[13] M. L. Perlman and G. Friedlander, Phys. Rev. 72, 1272 (1947); 74, 442 (1948).

change, especially increase, at higher energies. More likely, the slightly higher value obtained at Iowa State reflects a difference in experimental conditions; namely, the authors used a less attenuated beam which was relatively richer in low-energy quanta than the beam used by Katz and his co-workers. It seems, then, that the cross-section ratio for the Br^{80} isomers remains constant at higher energies. Both cross sections may fall to zero in the neighborhood of 30 Mev, or decrease to small values.

ACKNOWLEDGMENTS

Differential Cross Sections for the Scattering of Medium Energy Protons on Carbon*

Robert W. Peelle†

Palmer Physical Laboratory, Princeton University, Princeton, New Jersey

(Received August 31, 1956)

Extensive experimental results are presented showing the variation with energy of the absolute angular distributions for the elastic and inelastic scattering of medium energy protons on carbon. For the scattering with $Q=0$ and $Q=-4.4$ Mev, angular distributions between 20 deg and 170 deg were obtained for eleven incident proton energies spaced between 14.0 Mev and 19.4 Mev. Distributions for scattering leading to the excitation of the 7.7-Mev and 9.6-Mev states of C^{12} were measured at energies of 16.7, 17.8, and 18.9 Mev. The experimental results are discussed qualitatively in their relation to the predictions of the theories of nuclear reactions. The elastic scattering cross sections are roughly what one might expect from the complex potential

theory, but no numerical comparisons have been made. The predominant inelastic scattering is forward, though the angular distributions corresponding to the three levels studied do not resemble each other. In no single case is one of these distributions symmetrical about 90 deg. The simple Bessel-function distributions of the first-order direct interaction theory do not agree well with the data, but only the scattering leading to the 4.4-Mev level of C^{12} is in apparently complete disagreement.

Experimental differential cross sections as a function of energy are also presented for the scattering of protons on hydrogen near 90 deg (center-of-mass system).

1. INTRODUCTION

THE present work is a study of the variation with incident beam energy of the differential cross sections for the scattering of medium energy protons on carbon. Since this work was begun, some relevant experimental data[1-9] have become available for the scattering of protons from carbon, beryllium, oxygen, and neon.

† Present address: Oak Ridge National Laboratory, Post Office Box P, Oak Ridge, Tennessee.
[1] B. T. Wright, Phys. Rev. 82, 451 (1951).
[2] H. E. Gove and H. F. Stoddard, Phys. Rev. 86, 572 (1952).
[3] W. E. Burcham et al., Phys. Rev. 92, 1266 (1953).
[4] B. L. Cohen and R. V. Neidigh, Phys. Rev. 93, 282 (1954).
[5] G. E. Fischer, Phys. Rev. 96, 704 (1954).
[6] W. Hornyak and R. Sherr, Phys. Rev. 100, 1409 (1955).
[7] H. Conzett, Phys. Rev. 100, 1794 (A) (1955).
[8] I. Dayton and G. Schrank, Phys. Rev. 101, 1358 (1956). The data published by these authors for elastic scattering of 18.4-Mev protons on carbon are consistent with one of the measurements described here.
[9] J. Rotblat (private communication, 1956).

Measurements of the elastic scattering of medium energy protons on light nuclei are available in the works of Wright,[1] Burcham et al.,[3] Cohen and Neidigh,[4] Fischer,[5] Hornyak and Sherr,[6] Dayton and Schrank,[8] and Rotblat et al.[9] The results obtained have the appearance of arising from diffraction effects such as might be expected from complex-potential scattering, though no comparisons have been published. A reasonable fit in the case of a target nuclide of higher mass has been given by Woods and Saxon.[10] In such a case, the assumption of no compound-nuclear effects is thought to be more reasonable than for a light nuclide.

Inelastic proton scattering in the relevant energy and mass number regions has received less attention, partly because of the experimental difficulties in resolving particle groups from some light nuclides. Data corresponding to the 4.4-Mev level in carbon have been obtained by Gove and Stoddard,[2] Burcham et al.,[3] Fischer,[5] Conzett,[7] and Rotblat.[9] The results indicate

[10] R. D. Woods and D. S. Saxon, Phys. Rev. 95, 577 (1954).

some variation in the shape of the inelastic proton distributions over the incident proton energy interval between 7 and 12 Mev. Only at 10 Mev was forward-back symmetry observed in the center-of-mass (c.m.) system. A wide variety of inelastic scattering distributions for 19-Mev protons on oxygen has been demonstrated by Hornyak and Sherr.[6] The distribution for the 1.6-Mev level in Ne[20] has been investigated by Rotblat.[9]

The paucity of information concerning the variation with energy of the proton differential scattering cross sections made appropriate the experiment here described. Carbon was chosen as the target nuclide because of the ready availability of hydrocarbon foils, the supposedly closed-subshell character of the C^{12} ground state, the wide energy spacing of the first excited states of C^{12}, and the absence of experimental difficulties caused by particle groups corresponding to competing reactions.

The experimental program was planned to cover the variation with energy of the differential cross sections in sufficient detail that misinterpretation of the results would be unlikely. All possible steps consistent with this purpose were taken to promote confidence in the absolute cross sections.

2. APPARATUS

For this experiment the 60-in. scattering chamber described by Yntema and White[11] was used in conjunction with the Princeton synchrocyclotron. Fairly standard instrumentation was used, some details of which are given in the paragraphs below.

a. Production of the Focused Proton Beam

The excessively negative radial gradient of the Princeton cyclotron's magnetic field makes possible the alteration of the external beam energy over a fairly wide range without any change in the magnetic field shimming. The upper limit of the usable external beam energy at 19.4 Mev was set by failure of the oscillator system, while the lower limit was determined by a decrease in beam extraction efficiency which became increasingly important below about 15 Mev.

The external proton beam is focused by a combination of two thin magnetic lenses.[12] Beam focus adjustments were made with the help of fluorescent screens observable by telescope from the control console.

Beam energy stability was gained by the use of feedback control systems for the cyclotron magnet current, the electrostatic deflector voltage, and the focus magnet currents. Beam current stability was fair. An electrically actuated beam stopper within the cyclotron vacuum can was used to turn the external proton beam on and off without influencing any sensitive parameters of the accelerator.

b. Scattering Chamber

The 60-in. scattering chamber,[11] held at an air pressure of a few microns, contained the scattering foil, two scintillation detectors, and an aperture leading the unscattered proton beam to a charge-collecting cup. The proton beam incident upon the scattering foil was defined by two $\frac{1}{4}$-in. collimators spaced 32 in. apart, followed by a slightly larger antiscattering aperture. The second $\frac{1}{4}$-in. collimator was 22 in. from the scattering foil.

The scintillation detector used to measure the proton angular distributions was mounted on the rotatable bed within the scattering chamber. This detector could view protons scattered at any angle between −15 deg and 170 deg.

The second scintillation counter was stationed at a fixed angle of −30 deg to monitor the strength of the elastically scattered beam. This monitor provided important checks upon the operation of the current integrator and upon the thickness of the scattering foils.

Scattering foils were mounted on a probe assembly which allowed foil substitution without loss of vacuum. The foil orientation could be set within 0.2 deg of any desired angular position.

Protons of the unscattered beam were collected in the integrator cup described by Yntema and White.[11] The collected charge was measured electronically by using a circuit[13] whose calibration depended on a standardized dc potential and upon bridged input grid resistors.

c. Beam Energy Measurement

A virtually drift-free double proportional counter proton-range spectrometer[14] was used for measurements of the beam energy. In this device a differential range distribution in aluminum was obtained for protons scattered from the beam through an angle of 90 deg. For a given absorber thickness, only those scattered protons were counted whose range ended in the second of the proportional counters. Average beam energies, determined with the help of the range-energy relation of Bichsel and Mozley,[15] (see Table I) are felt to be accurate within 50 kev if error in the range-energy relation is neglected. The 50-kev error should be compared with an estimated intrinsic beam spread of about 0.2 Mev. Figure 1 shows typical differential range distributions obtained with this apparatus. The range spectrometer was positioned between the cyclotron and the collimators of the 60-in. scattering chamber, so it may have received an atypical sample of the beam. In practice, no differences in the experimental cross sections were observed after the beam energy had been reset with the aid of this instrument.

[11] J. L. Yntema and M. G. White, Phys. Rev. 95, 1226 (1954).
[12] F. C. Shoemaker et al., Phys. Rev. 86, 582 (A) (1952).
[13] This circuit was derived by W. A. Franzen from W. Higginbotham and S. Rankowitz, Rev. Sci. Instr. 22, 688 (1951).
[14] This spectrometer was designed and built in collaboration with J. B. Reynolds.
[15] H. Bichsel and R. Mozley (to be published).

d. Proton-Sensitive Scintillation Detectors

Thallium-activated sodium iodide scintillation crystals cleaved to dimensions of about $\frac{1}{8} \times \frac{1}{2} \times \frac{1}{2}$ in. were used for the energy-sensitive detection of scattered protons. These crystals were placed inside air-tight mountings having thin mica windows for penetration of the protons. A nonhardening polystyrene preparation[16] was used to provide optical matching at the interfaces between optically dense materials. The cross-section detector was contained within a sealed housing[17] operated at atmospheric pressure. The detector solid angle was defined by a collimator mounted external to this housing. When the cross-section detector was set at large scattering angles, an intense gamma-ray background was observed because of the proximity to the beam collimators. This background, which obscured proton groups in some cases, was effectively reduced by about a factor of thirty when the scintillation pulses were placed in coincidence with those from a proportional counter positioned between the scattering foil and the detector. The aperture of this conventional counter[17] was kept somewhat larger than that of the collimator over the crystal. The total thickness of this counter, including mica foils to contain the counting gas, was about 5 mg/cm^2.

e. Pulse-Height Spectrometry

A block diagram of all the electronic equipment associated with the scintillation detectors is given in Fig. 2. The cross-section measurements depended directly upon the differential pulse-height analysis furnished by a Bell and Kelley[18] type analyzer. This analyzer possessed adequate resolution, the provisions for coincidence gating required by the gamma-ray suppressing proportional counter, a known short dead-time, and a most important freedom from gap and overlap regions between successive channels.

3. EXPERIMENTAL METHOD

The experimental method consisted of procedures both to insure proper operation of the apparatus, and to accumulate data. The latter were quite simple when only those proton groups were observed corresponding to elastic scattering and excitation of the 4.4-Mev level. In these cases the angular distributions at a single incident energy were obtained without interruption. When the excitations of the 7.7- and 9.6-Mev levels of C^{12} were observed, the experiment was complicated by the need to operate about two weeks for the acquisition of a single set of distributions.

Daily checks were made on all crucial properties of the electronic instrumentation. When it was desired

[16] R. L. Shipp, Rev. Sci. Instr. **23**, 773 (1952).
[17] Designed and built by K. G. Standing. See Fig. 1 of K. G. Standing, Phys. Rev. **101**, 152 (1956).
[18] Described by A. B. Van Rennes, Nucleonics **10**, No. 10, 50 (1952).
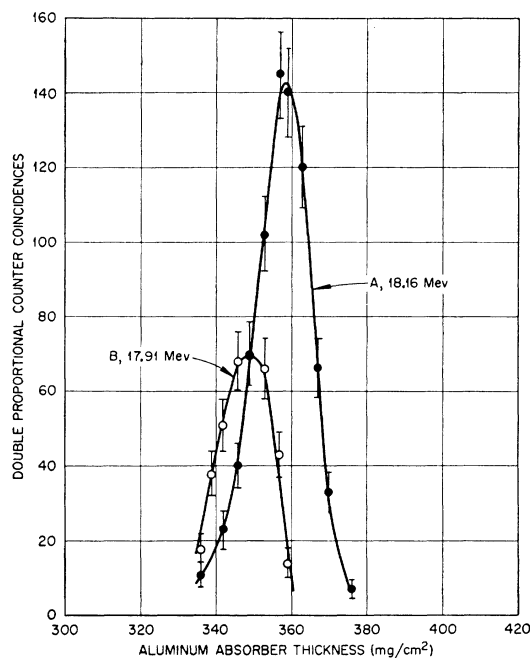
FIG. 1. Sample differential range distributions. Curve A represents data taken during the original testing of the double proportional counter range spectrometer. Curve B, taken a number of months later, is a typical curve of the type obtained daily for measurement of the average beam energy. The energies quoted are the mean proton beam energies established by these curves, and are believed accurate within the estimated standard deviation of 0.05 Mev. The ability of the device to detect an energy difference of about 0.25 Mev is illustrated by this figure.

to repeat a previously used beam energy, the magnetic field was adjusted until the differential range straggling curve appeared identical to that recorded for the earlier run. During a given day's run, repetitive checks on the cyclotron parameters and the current integrator calibration were interspersed between measurements.

At each scattering angle where a cross section was measured, the following were recorded: the pulse-height spectrum in the neighborhood of the desired group, the number of elastically scattered protons observed in the −30-deg monitor, and the charge collected in the integrator cup during the time required for the spectral measurement. Successive scattering angles were staggered to show up possible equipment drifts, and repeated points were obtained whenever the experimental geometry was changed. The counting time for each measurement was adjusted so that the statistical error in the number of counts obtained should be roughly similar in magnitude to the error originating in the subtraction of background from the experimental pulse spectrum.

Cross sections for proton scattering from hydrogen in the hydrocarbon foils were measured for at least two angles at each incident beam energy. Great care was not taken with these data, because further understanding

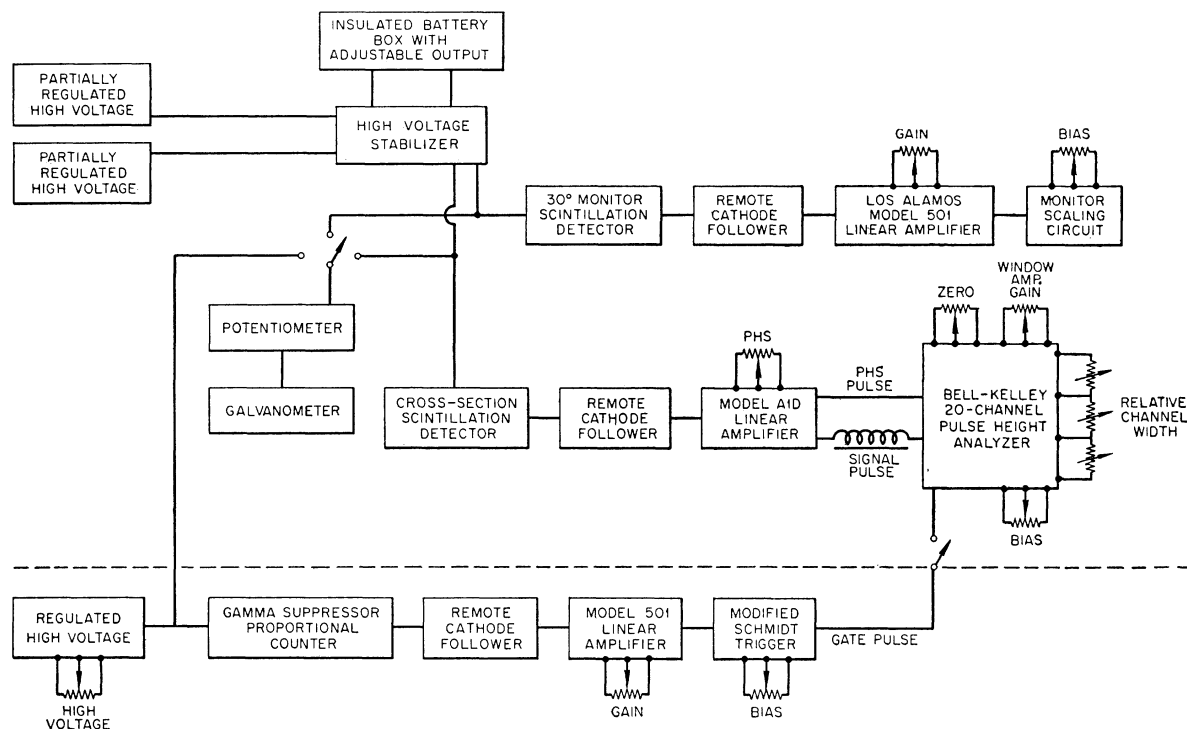Fig. 2. A block diagram of the electronic equipment associated with the −30-deg monitor, the cross-section detector, and the gamma-ray-suppressing proportional counter. The "high-voltage stabilizer" for each desired high-voltage output consisted of a type 7B4 triode operating as a cathode follower with the battery potential on its grid and the bleeder for the photomultiplier dynode voltages as its load. Because of a shortage of scaling circuits, the 20-channel analyzer had only fifteen channels in operation during most of the experiment.

of the p-p interaction requires precision measurements considered outside the province of this work.

4. ANALYSIS OF THE DATA

This section describes the methods used to process the raw data, the corrections applied, and the known experimental errors. Tables of results are presented and explained.

a. Energy of the Incident Proton Beam

The range in aluminum of protons scattered through 90 deg by carbon was obtained directly from the peak

Table I. An experimental relationship between proton energy and mean range in aluminum, from the work of Bichsel and Mozley.[15] Estimated errors in both energy and range are supposed to be about 0.2%.

Energy Mev	Range mg/cm²	Energy Mev	Range mg/cm²
8.00	114.8	15.00	343.9
9.00	140.7	16.00	385.2
10.00	169.0	17.00	428.5
11.00	199.3	18.00	473.9
12.00	232.2	19.00	521.4
13.00	267.3	20.00	570.9
14.00	304.7		

position of the differential range spectrum, after correction for the stopping power of the range spectrometer assembly. The proton energy corresponding to this range was determined from the data of Table I, and the unscattered beam energy then obtained by the use of Newtonian scattering energetics. The energies and errors given with the tables of data take into account the thickness and angular position of the scattering foil in the 60-in. scattering chamber.

b. Subtraction of Background

Figure 3 shows three typical pulse-height spectra obtained from the cross section detector. The total number of pulses within any one of the proton groups could not be ascertained until the apparent continuum was subtracted as a background. This continuum arose largely from slit scattering off the collimator defining the detector solid angle. Since no completely reliable method was available for a quantitative determination of the background at the energy of a given proton group, the simple recipe illustrated by the dotted lines in Fig. 3 was adopted to insure consistency. In each individual case an estimated probable error was assigned to this background, commensurate with the extent to which its value appeared uncertain.
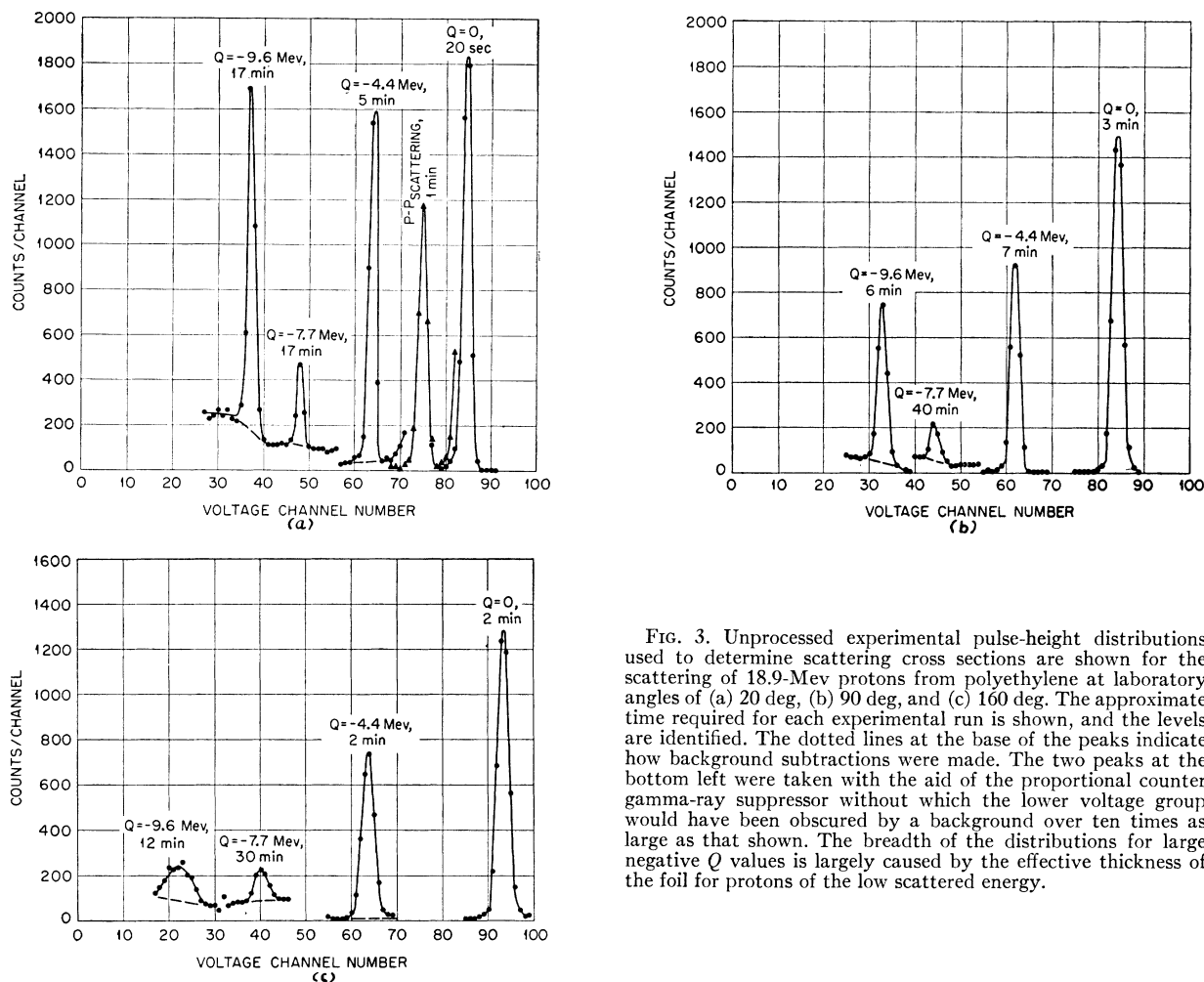
FIG. 3. Unprocessed experimental pulse-height distributions used to determine scattering cross sections are shown for the scattering of 18.9-Mev protons from polyethylene at laboratory angles of (a) 20 deg, (b) 90 deg, and (c) 160 deg. The approximate time required for each experimental run is shown, and the levels are identified. The dotted lines at the base of the peaks indicate how background subtractions were made. The two peaks at the bottom left were taken with the aid of the proportional counter gamma-ray suppressor without which the lower voltage group would have been obscured by a background over ten times as large as that shown. The breadth of the distributions for large negative Q values is largely caused by the effective thickness of the foil for protons of the low scattered energy.

c. Calculation of the Differential Cross Sections

Uncorrected laboratory cross sections were calculated[19] with the use of foil surface densities obtained by weighing the central area of each foil and by assuming that the polyethylene and polystyrene foils had the chemical compositions indicated by their formulas. The paragraphs below describe corrections applied to the cross sections so calculated.

Zero-angle corrections.—Three sources of information were used to obtain values of the true zero of scattering angle: data taken with the cross-section detector at small negative scattering angles, the counting rate in the −30-deg monitor compared to that of the cross section detector at similar positive angles, and observations of the energy of the p-p scattering proton group. The three methods did not yield completely consistent

results, but all indicated a maximum correction of about one degree. Since a slight time dependence was apparent, the first part of the data was corrected by 0.3 deg and the second part by 0.9 deg.

Foil thickness correction.—The surface densities of the ten foils used in this experiment were obtained by weighing, but they were also interrelated in pairs by ratios obtained from relative scattering yields observed in the monitor detector. A graphical solution was found for the resulting doubly overdetermined set of equations in the foil surface densities.

Three of the foils were of such nonuniform thickness that the above method gave no solution. In these cases the surface density was finally based on the smoothness of the p-p scattering cross section as a function of energy. Since the three nonuniform foils were used near the center of the energy range covered, the actual energy dependence of the p-p cross section matters little for this normalization.

Counting loss corrections.—Some of the pulse-height spectra measured at small scattering angles were sub-

---

[19] The standard zero-order consideration of the geometrical scattering problem was used to calculate the cross sections. Trial application of the more exact formula given in the appendix of Dayton and Schrank[8] indicates that this practice was fully justified.

TABLE II. A summary of the notation and units used in the tabulations of results.

Symbol	Definition
T_i(Mev)	mean incident proton energy at the center of the scattering foil, lab system[a]
ΔT_i(Mev)	estimated standard deviation[b] in the mean incident energy
θ(deg)	c.m. mean scattering angle
$\Delta\theta$(deg)	estimated standard deviation in θ
δ(deg)	root-mean-square angular deviation from the quoted scattering angle[c]
$\sigma(\theta)$ (mb/sterad)	c.m. differential cross section at θ
$\Delta_a\sigma$ (mb/sterad)	estimated standard deviation associated with a given measurement of $\sigma(\theta)$
$\Delta_{na}\sigma/\sigma$	estimated relative standard deviation representative of an entire angular distribution
$-Q$(Mev)	excitation energy of the residual nucleus

[a] C.m. proton energies for scattering from C^{12} are equal to 0.923 times the laboratory energies given.
[b] Since this estimate includes uncertainty in the aluminum absorber thickness, incident energy settings could be repeated within a tolerance smaller than ΔT_i.
[c] This deviation was calculated from the magnitude of the beam size and detector collimator aperture in relation to the distance from scattering foil to detector.

TABLE III. A summary of incident energies, root-mean-square angular deviations, and errors. A "run" consists of the set of elastic and inelastic distributions measured concurrently at a given incident proton energy. The notation used here is defined in Table II.

Run No.[a]	T_i	ΔT_i	$\Delta\theta$	δ[b]	$\Delta_{na}\sigma/\sigma$
1	13.97	0.08	0.5	1.1	0.024
2	14.66	0.07	0.5	1.1	0.024
3	15.22	0.07	0.5	1.1	0.024
4	15.59	0.07	0.5	1.1	0.024
5	16.23	0.07	0.5	0.8	0.019
6	16.68	0.07	0.5	0.8	0.020
7[c]	16.72	0.07	0.5	1.2	0.024
8[d]	17.36	0.07	0.5	0.8	0.037
9[c]	17.75	0.07	0.5	1.2	0.023
10[d]	17.91	0.07	0.5	0.8	0.043
11[d]	18.40	0.07	0.5	0.8	0.043
12[c]	18.88	0.08	0.5	0.9	0.022
13	18.90	0.07	0.5	0.7	0.020
14	19.42	0.07	0.5	1.3	0.020

[a] The runs are ordered in sequence of increasing energy.
[b] The quoted values of this deviation are the largest typical calculated values for the given distribution.
[c] This run included distributions for inelastic scattering leading to the 7.7- and 9.6-Mev levels of C^{12}.
[d] The absolute cross section for this run was normalized with the help of p-p scattering data. See Sec. 4c of the text.

ject to counting losses as large as 7%. Rough corrections were calculated on the basis of the observed counting rate, the pulse-height analyzer dead-time, and the gross duty cycle of the synchrocyclotron. One-third of the total correction was taken as the estimated error in the correction.

d. Discussion and Classification of Errors

Uncertainty in the scattering angles.—The estimated standard deviation of 0.5 deg quoted on all scattering angle measurements was compounded from three sources: the uncertainty in the zero-angle correction discussed in Sec. 4c, the estimated error in the alignment of the collimator on the scintillation detector, and the estimated extent to which the center of gravity of the proton beam may have missed the axis of the scattering chamber table.

Uncertainty in the cross sections.—All recognized errors in the cross sections have been analyzed and reported in two separate categories. "Associated" errors are those largely associated with a given differential cross section, and may distort the shape of a distribution. "Nonassociated" errors are those which influence the absolute value of an entire angular distribution. The total estimated standard deviation in the absolute value of a single differential cross section may be determined by combining the quoted values of the associated and nonassociated standard deviations for that cross section.

The associated errors quoted for each cross section include allowances for the statistical error in the number of pulses counted, the estimated error in the subtraction of the background continuum, the estimated error in the counting-loss correction, and the estimated error in the counting time. Though the last three of

these errors are not truly random, all were combined as if they represented normal distributions.

The recognized sources of nonassociated error include failure of the current integrator system, lack of knowledge of the exact scattering geometry, and uncertainties in the surface densities of the scattering foils. These errors were estimated for each distribution and combined as the sums of squares.

e. Tabular Presentation of Results

Table II gives the notation and units used in the remainder of the data tables. Table III defines the ordering of the data, and lists all those parameters which are identified with the run at a given energy. Tables IV and V give the data obtained for elastic scattering and excitation of the 4.4-Mev level at the fourteen incident energies used. Tables VI and VII list data for excitation of the 7.7- and 9.6-Mev levels at the three energies where they were observed. Table VIII presents integrated partial cross sections for inelastic scattering leading to each of the studied states of C^{12}.

5. DISCUSSION OF RESULTS

Sections 5a through 5d deal with the energy dependence of the differential cross section measurements. Section 5e discusses the results of p-p scattering at 90-deg c.m. in the medium energy range.

a. Protons on Carbon, $Q = 0$

Figure 4, a comparison of representative results for elastic proton scattering on carbon, shows the trend of this angular distribution as the incident energy is varied. The gross effect is that which would be ex-

TABLE IV. Differential cross sections for the elastic scattering of protons on carbon. See Table II for notation and Table III for relevant experimental parameters. Where individual cross sections were measured more than once, the values presented are averages weighted according to the corresponding associated standard deviations.

Run 1, $T_i = 14.0$ Mev

θ	$\sigma(\theta)$	$\Delta_a\sigma$	θ	$\sigma(\theta)$	$\Delta_a\sigma$
20.4	548	10	95.7	22.1	0.6
22.6	476	9	105.6	27.3	1.0
29.1	313	7	115.4	26.3	1.1
35.3	207	7	125.0	22.9	0.9
44.1	106	4	134.5	16.8	0.7
54.6	38.2	1.8	143.9	10.9	0.5
65.1	7.05	0.42	153.2	7.6	0.3
75.5	7.96	0.29	162.4	6.7	0.3
85.6	14.4	0.4	171.6	7.6	0.3

Run 2, $T_i = 14.7$ Mev

θ	$\sigma(\theta)$	$\Delta_a\sigma$	θ	$\sigma(\theta)$	$\Delta_a\sigma$
20.4	615	9	95.7	28.0	0.4
22.6	535	8	105.6	30.7	0.9
30.2	329	5	115.4	28.8	0.6
36.6	212	3	125.0	24.9	0.6
44.1	109	3	134.5	17.6	0.5
54.6	33.3	0.3	143.9	13.2	0.4
59.9	17.2	0.5	153.2	7.5	0.3
65.1	10.7	0.4	162.4	5.75	0.19
70.3	9.8	0.3	167.0	4.74	0.24
75.4	13.3	0.3	171.7	4.90	0.14
85.6	22.1	0.3			

Run 3, $T_i = 15.2$ Mev

θ	$\sigma(\theta)$	$\Delta_a\sigma$	θ	$\sigma(\theta)$	$\Delta_a\sigma$
20.5	621	12	95.7	25.7	0.4
22.6	551	11	100.7	27.1	0.6
30.2	351	6	105.6	30.2	0.6
33.4	276	5	110.5	29.5	0.6
44.1	109	2	115.4	27.7	0.6
49.4	59.0	1.2	120.2	24.2	0.6
54.6	30.4	0.6	125.0	24.1	0.6
59.9	15.7	0.4	134.5	18.4	0.5
65.1	9.73	0.3	143.9	13.3	0.4
70.3	9.46	0.2	153.2	10.0	0.2
75.5	12.4	0.3	162.4	9.0	0.2
85.6	20.0	0.4	167.0	9.4	0.3
			171.6	10.3	0.3

Run 4, $T_i = 15.6$ Mev

θ	$\sigma(\theta)$	$\Delta_a\sigma$	θ	$\sigma(\theta)$	$\Delta_a\sigma$
20.4	618	21	85.6	20.6	0.5
22.6	520	12	95.7	27.8	0.4
29.1	359	8	105.6	31.0	0.6
33.4	275	4	115.4	27.6	0.6
44.1	115	1.3	125.0	22.9	0.6
54.6	34.3	0.9	134.5	16.9	0.3
59.9	17.4	0.5	143.9	12.2	0.3
65.1	10.9	0.3	153.3	9.33	0.24
70.3	9.94	0.24	162.4	9.54	0.18
75.4	12.5	0.3	167.0	9.74	0.25
			171.6	10.2	0.3

Run 5, $T_i = 16.2$ Mev

θ	$\sigma(\theta)$	$\Delta_a\sigma$	θ	$\sigma(\theta)$	$\Delta_a\sigma$
19.9	615	10	80.1	17.7	0.3
22.1	547	8	85.1	22.8	0.3
26.3	442	6	95.2	29.3	0.3
32.9	294	3	100.2	30.4	0.3
39.3	184	3	105.1	32.0	0.4
43.5	123	2	114.9	28.1	0.4
48.8	73.7	1.2	124.5	21.6	0.4
54.1	40.1	0.8	134.0	16.3	0.3
59.4	22.0	0.5	143.4	10.8	0.2
64.6	13.3	0.3	152.8	9.14	0.14
69.8	11.5	0.3	162.0	9.90	0.25
74.9	13.7	0.2	166.6	10.6	0.3
			171.2	12.4	0.3

Run 6, $T_i = 16.7$ Mev

θ	$\sigma(\theta)$	$\Delta_a\sigma$	θ	$\sigma(\theta)$	$\Delta_a\sigma$
22.1	586	21	85.1	20.5	0.3
26.4	443	7	95.2	26.5	0.4
32.9	284	5	105.1	27.6	0.2
40.5	165	3	114.9	24.4	0.3
43.5	118	2	124.5	18.9	0.3
48.2	68.3	1.1	134.1	12.7	0.3
50.9	55.5	1.5	143.8	8.91	0.21
54.1	37.1	0.7	152.8	8.29	0.21
59.4	19.8	0.4	162.0	10.6	0.2
64.6	12.9	0.3	166.6	11.3	0.2
69.7	11.7	0.2	171.2	13.0	0.3
74.9	13.7	0.2			

Run 7, $T_i = 16.7$ Mev

θ	$\sigma(\theta)$	$\Delta_a\sigma$	θ	$\sigma(\theta)$	$\Delta_a\sigma$
17.7	689	12	85.1	22.6	0.5
22.1	555	7	95.2	25.3	0.3
26.4	432	8	114.9	24.8	0.3
32.9	272	6	124.5	17.9	0.2
37.1	198	3	134.0	12.6	0.3
40.3	155	3	143.4	8.32	0.16
48.8	66.2	0.5	152.7	7.46	0.13
59.4	19.0	0.4	161.9	9.53	0.13
64.6	12.5	0.2	171.2	13.1	0.2
74.9	15.2	0.3			

Run 8, $T_i = 17.4$ Mev

θ	$\sigma(\theta)$	$\Delta_a\sigma$	θ	$\sigma(\theta)$	$\Delta_a\sigma$
22.1	447	14	85.1	17.7	0.3
26.4	349	7	95.2	22.1	0.3
32.9	246	4	100.2	23.6	0.4
39.2	148	2	105.1	23.8	0.4
43.5	98.5	1.7	114.9	22.2	0.4
48.8	59.4	1.1	124.5	15.6	0.4
54.1	32.8	0.5	134.0	10.3	0.2
59.4	18.2	0.4	142.9	7.60	0.12
64.6	11.3	0.3	148.1	7.00	0.22
69.8	10.6	0.2	152.8	7.64	0.28
74.9	12.0	0.2	162.0	10.0	0.2
80.1	14.8	0.3	166.6	11.2	0.3
			171.2	12.3	0.2

Run 9, $T_i = 17.8$ Mev

θ	$\sigma(\theta)$	$\Delta_a\sigma$	θ	$\sigma(\theta)$	$\Delta_a\sigma$
17.1	663	19	95.7	22.5	0.2
22.5	515	9	105.7	20.9	0.2
28.0	440	6	115.4	16.8	0.2
33.4	269	4	125.0	10.8	0.1
39.7	160	3	134.6	6.48	0.1
44.0	109	3	143.9	5.55	0.06
54.6	32.5	0.8	153.3	7.80	0.11
65.1	14.6	0.3	162.5	14.0	0.1
75.4	16.1	0.2	171.7	19.1	0.2
85.7	20.5	0.3			

Run 10, $T_i = 17.9$ Mev

θ	$\sigma(\theta)$	$\Delta_a\sigma$	θ	$\sigma(\theta)$	$\Delta_a\sigma$
22.1	422	14	85.1	19.4	0.4
26.4	365	12	95.2	20.7	0.2
32.9	248	6	100.2	19.2	0.6
39.3	150	3	105.1	18.9	0.2
43.5	101	2	114.9	14.6	0.4
48.8	57.1	0.3	124.5	9.12	0.21
54.1	31.2	0.6	134.0	4.45	0.09
59.4	18.0	0.4	143.4	3.17	0.11
64.6	13.1	0.3	148.1	3.75	0.23
69.8	13.3	0.2	152.8	5.42	0.25
74.9	15.0	0.3	162.0	10.2	0.2
80.1	17.7	0.4	166.6	12.7	0.3
			171.2	14.7	0.3

ROBERT W. PEELLE

TABLE IV—*Continued.*

Run 11, $T_i = 18.4$ Mev

θ	$\sigma(\theta)$	$\Delta_a\sigma$	θ	$\sigma(\theta)$	$\Delta_a\sigma$
22.1	506	19	85.1	19.5	0.2
26.0	404	12	95.2	21.8	0.1
32.8	264	5	105.1	20.7	0.2
39.2	161	4	114.9	16.0	0.3
43.5	104	2	124.5	10.3	0.2
48.8	59.9	0.4	134.1	4.75	0.10
54.1	33.0	0.6	144.4	2.58	0.12
59.4	19.1	0.4	152.8	4.24	0.20
64.6	14.7	0.4	162.0	9.50	0.22
69.8	13.6	0.4	166.6	11.7	0.1
74.9	15.3	0.4	171.2	14.1	0.3

Run 12, $T_i = 18.9$ Mev

θ	$\sigma(\theta)$	$\Delta_a\sigma$	θ	$\sigma(\theta)$	$\Delta_a\sigma$
13.4	1038	27	74.9	19.7	0.2
17.7	768	5	85.1	21.8	0.2
22.0	644	22	95.2	22.8	0.1
26.4	444	7	105.1	23.2	0.2
32.8	283	3	113.9	20.2	0.2
38.2	204	4	124.6	12.8	0.2
43.5	114	1	134.1	5.48	0.06
48.8	63.7	1.0	143.2	2.36	0.04
54.1	35.7	0.6	152.8	4.66	0.06
64.6	18.8	0.2	162.0	11.6	0.2
			166.6	14.3	0.2
			173.0	20.1	0.2

Run 13, $T_i = 18.9$ Mev

θ	$\sigma(\theta)$	$\Delta_a\sigma$	θ	$\sigma(\theta)$	$\Delta_a\sigma$
26.4	460	8	105.1	22.5	0.3
32.8	310	8	114.9	19.3	0.4
40.3	156	3	124.6	12.2	0.3
48.8	66.3	1.3	134.1	5.66	0.17
54.1	34.2	0.6	138.8	3.49	0.16
59.4	22.7	0.6	143.4	2.48	0.17
64.6	17.3	0.4	148.1	3.03	0.21
69.8	18.1	0.4	152.8	4.97	0.20
74.9	18.7	0.3	162.0	10.4	0.2
85.1	19.9	0.3	166.6	15.0	0.3
95.2	22.8	0.3	171.2	18.8	0.4

Run 14, $T_i = 19.4$ Mev

θ	$\sigma(\theta)$	$\Delta_a\sigma$	θ	$\sigma(\theta)$	$\Delta_a\sigma$
17.7	818	24	85.2	22.4	0.4
18.8	768	22	90.2	20.1	0.4
26.4	527	9	95.2	20.2	0.5
32.8	319	3	105.2	14.8	0.2
39.2	175	2	114.9	12.3	0.3
43.5	112	2	124.6	9.21	0.09
48.8	59.0	1.1	134.1	6.72	0.18
54.1	28.9	0.5	143.5	4.82	0.09
59.4	18.1	0.3	148.2	4.36	0.10
64.7	16.6	0.3	152.8	4.70	0.11
69.8	18.2	0.3	162.1	7.00	0.16
74.9	21.1	0.3	171.2	8.95	0.14
80.1	23.1	0.4			

pected if the scattering were well represented by a complex potential. Fitting a complex potential well to nuclides as light as carbon has been generally avoided because of fear that compound elastic scattering might produce important interference effects. The qualitative features of the data near 18.0 Mev suggest that if the distributions in that energy region could be fitted with a complex potential, the parameters of the fit might be forced to change rather rapidly with energy. Such a rapid change would negate some of the value of the complex potential representation.
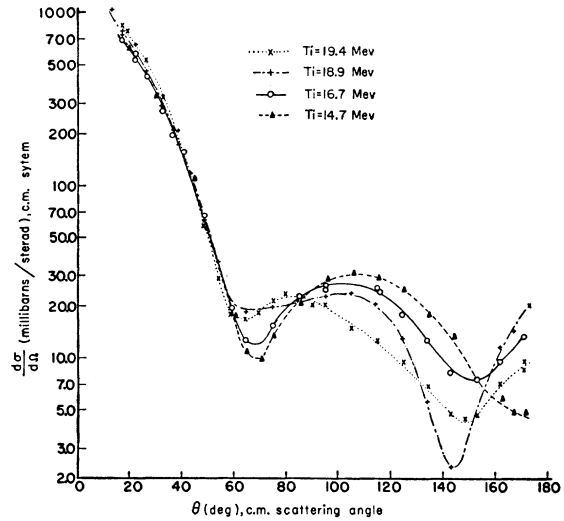

FIG. 4. $C^{12}(p,p)C^{12}$. This plot presents four of the measured differential cross sections for the elastic scattering of protons on carbon. The associated estimated standard deviations peculiar to a point are the size of that point. The curves are drawn primarily to connect points measured at the same incident proton laboratory energy.

b. Protons on Carbon, $Q = -4.4$ Mev

Figure 5 shows typical results for inelastic scattering leading to the 4.4-Mev level of C^{12}. At no point between 14.0 and 19.4 Mev was an energy found for which these scattering cross sections were symmetrical about 90 deg. The curves shown indicate the general character of all those obtained; they exhibit a marked minor variation in shape. The forwardness of the scattering appears to become slightly more pronounced at the higher energies.

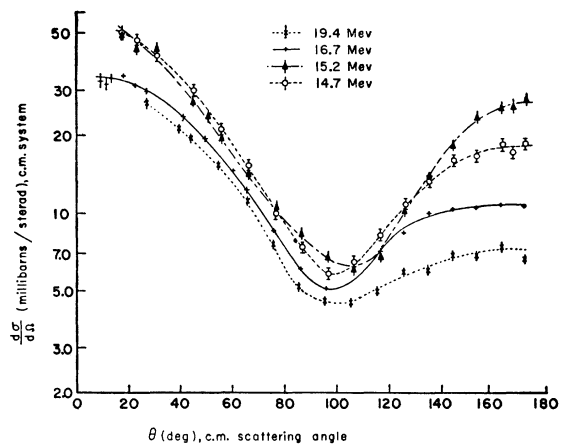FIG. 5. $C^{12}(p,p')C^{12*}$, $Q = -4.4$ Mev. A plot of representative data on the differential inelastic scattering cross sections for protons on C^{12} with $Q = -4.4$ Mev. Representative associated standard deviations are shown for certain measured points. The curves are drawn primarily to connect points measured at the same incident proton laboratory energy.

TABLE V. Differential cross sections for excitation of the 4.4-Mev level of C^{12} by proton inelastic scattering. See Table II for notation and Table III for relevant experimental parameters. Repeated measurements are represented by weighted averages.

Run 1, $T_i=14.0$ Mev

θ	$\sigma(\theta)$	$\Delta_a\sigma$	θ	$\sigma(\theta)$	$\Delta_a\sigma$
17.6	60	2	96.8	7.3	0.6
23.1	52	2	106.7	8.6	0.5
29.6	43.4	2.5	116.4	9.3	0.5
44.8	23.8	3.9	125.9	10.5	0.6
55.5	24.0	0.8	135.3	12.1	0.7
66.1	16.9	0.8	144.6	16.3	0.5
76.5	11.8	0.8	153.7	21.0	0.7
86.6	8.7	0.4	162.8	21.5	0.9
			171.8	27.3	1.0

Run 2, $T_i=14.7$ Mev

θ	$\sigma(\theta)$	$\Delta_a\sigma$	θ	$\sigma(\theta)$	$\Delta_a\sigma$
17.5	49.7	1.7	106.6	6.50	0.20
23.1	46.2	1.3	116.4	8.27	0.27
30.6	40.6	1.0	125.9	10.8	0.3
44.7	29.9	1.0	135.3	13.3	0.4
55.4	21.2	0.7	144.6	16.1	0.5
66.0	15.3	0.6	153.7	16.7	0.5
76.4	10.0	0.3	162.8	18.6	0.5
86.7	7.40	0.24	167.3	17.3	0.5
96.7	5.81	0.20	171.8	18.6	0.6

Run 3, $T_i=15.2$ Mev

θ	$\sigma(\theta)$	$\Delta_a\sigma$	θ	$\sigma(\theta)$	$\Delta_a\sigma$
17.5	49.3	2.1	96.7	6.68	0.20
23.1	43.9	1.5	106.6	6.19	0.15
30.6	42.2	1.1	116.3	6.71	0.21
44.7	26.9	0.7	125.8	10.4	0.3
50.1	23.8	0.6	135.3	13.9	0.2
55.4	19.2	0.5	144.5	18.2	0.3
66.0	14.2	0.3	153.7	23.3	0.6
76.4	10.3	0.3	162.7	25.6	0.6
86.6	8.21	0.24	167.3	25.7	0.6
			171.8	27.3	0.6

Run 4, $T_i=15.6$ Mev

θ	$\sigma(\theta)$	$\Delta_a\sigma$	θ	$\sigma(\theta)$	$\Delta_a\sigma$
17.5	48.1	2.2	106.5	6.78	0.15
23.0	45.3	1.6	116.2	7.96	0.22
29.5	39.4	1.1	125.8	10.5	0.3
44.7	25.7	0.7	135.2	12.2	0.3
55.3	18.7	0.5	144.5	15.1	0.5
65.9	13.0	0.3	154.1	17.8	0.5
71.2	10.9	0.3	162.7	21.1	0.6
76.3	9.52	0.21	167.3	20.9	0.4
86.6	6.88	0.22	171.8	21.2	0.6
96.6	6.32	0.12			

Run 5, $T_i=16.2$ Mev

θ	$\sigma(\theta)$	$\Delta_a\sigma$	θ	$\sigma(\theta)$	$\Delta_a\sigma$
22.4	38.1	1.4	106.0	6.31	0.16
26.8	35.4	1.3	115.7	7.57	0.25
40.9	29.1	0.8	125.3	9.44	0.21
44.1	26.2	1.0	134.7	11.7	0.3
54.8	19.8	0.6	144.0	13.2	0.4
65.4	12.5	0.4	153.2	13.2	0.5
75.8	8.99	0.22	162.3	15.1	0.5
86.1	5.92	0.21	166.8	13.7	0.6
96.1	5.82	0.14	171.3	14.5	0.7

Run 6, $T_i=16.7$ Mev

θ	$\sigma(\theta)$	$\Delta_a\sigma$	θ	$\sigma(\theta)$	$\Delta_a\sigma$
22.5	33.4	1.2	106.0	6.09	0.18
26.9	31.5	1.4	116.0	7.19	0.22
41.0	22.9	0.9	125.5	8.56	0.23
44.3	25.3	0.6	134.9	10.0	0.3
55.0	17.7	0.4	144.2	11.6	0.3
65.6	11.8	0.3	153.3	11.7	0.4
76.0	8.45	0.19	162.4	13.0	0.4
86.2	6.36	0.24	166.9	12.6	0.4
96.3	5.20	0.17	171.4	12.3	0.4

Run 7, $T_i=16.7$ Mev

θ	$\sigma(\theta)$	$\Delta_a\sigma$	θ	$\sigma(\theta)$	$\Delta_a\sigma$
9.2	32.3	2.0	75.8	8.55	0.16
11.4	31.6	2.0	86.0	6.09	0.17
13.6	33.2	1.5	96.1	5.09	0.11
18.0	34.1	0.9	116.0	7.11	0.13
22.4	31.2	0.8	125.3	8.39	0.21
26.8	29.7	1.0	134.7	10.1	0.15
40.9	23.7	0.9	144.0	10.4	0.2
49.5	19.5	0.4	153.2	11.2	0.2
60.0	14.6	0.3	162.3	11.9	0.3
65.4	12.3	0.3	171.3	11.4	0.3

Run 8, $T_i=17.4$ Mev

θ	$\sigma(\theta)$	$\Delta_a\sigma$	θ	$\sigma(\theta)$	$\Delta_a\sigma$
22.4	26.8	1.1	106.0	4.64	0.12
26.7	25.4	1.1	115.7	5.82	0.17
39.8	20.5	0.5	125.2	7.26	0.20
44.1	19.8	0.7	134.7	8.91	0.29
54.7	15.9	0.4	144.0	9.93	0.27
65.3	11.1	0.2	153.2	12.4	0.3
75.7	7.16	0.10	162.3	12.7	0.4
86.0	4.87	0.12	166.8	13.2	0.4
96.0	4.91	0.13	171.3	13.4	0.2

Run 9, $T_i=17.8$ Mev

θ	$\sigma(\theta)$	$\Delta_a\sigma$	θ	$\sigma(\theta)$	$\Delta_a\sigma$
11.9	25.5	2.0	86.4	5.43	0.11
17.4	32.3	0.9	96.5	4.16	0.05
22.8	30.7	0.9	106.4	4.01	0.06
28.2	31.4	0.9	116.2	4.80	0.09
40.2	24.1	0.7	125.7	5.82	0.07
44.4	24.1	0.5	135.1	7.20	0.10
55.2	18.8	0.5	144.4	7.79	0.11
65.7	12.9	0.3	153.6	9.05	0.12
76.1	8.61	0.12	162.7	10.5	0.12
			171.8	11.0	0.13

Run 10, $T_i=17.9$ Mev

θ	$\sigma(\theta)$	$\Delta_a\sigma$	θ	$\sigma(\theta)$	$\Delta_a\sigma$
22.4	29.2	1.4	96.0	3.74	0.11
26.7	27.6	1.1	105.9	3.64	0.11
39.7	23.4	0.6	115.6	4.18	0.11
44.0	21.8	0.6	125.2	4.71	0.13
49.4	18.7	0.5	134.6	5.83	0.20
54.7	16.8	0.4	144.0	6.98	0.25
65.3	11.7	0.3	153.2	7.33	0.23
75.7	8.02	0.21	162.3	7.72	0.23
85.9	5.22	0.16	166.8	8.19	0.33
			171.3	8.43	0.29

Run 11, $T_i=18.4$ Mev

θ	$\sigma(\theta)$	$\Delta_a\sigma$	θ	$\sigma(\theta)$	$\Delta_a\sigma$
22.4	24.0	1.4	96.0	4.89	0.18
26.8	24.1	1.1	105.9	4.13	0.10
39.7	21.1	0.6	115.7	4.37	0.17
44.0	18.8	0.6	125.2	4.58	0.13
49.4	18.1	0.7	134.7	5.33	0.18
54.7	15.8	0.4	144.0	6.45	0.22
65.3	12.0	0.4	153.2	6.75	0.38
75.7	8.23	0.23	162.3	8.06	0.28
85.9	5.86	0.11	171.3	8.52	0.28

Run 12, $T_i=18.9$ Mev

θ	$\sigma(\theta)$	$\Delta_a\sigma$	θ	$\sigma(\theta)$	$\Delta_a\sigma$
9.2	17.8	1.6	85.8	5.55	0.06
13.5	25.3	1.0	96.0	4.80	0.07
17.9	25.4	0.3	105.8	5.17	0.07
22.3	26.7	0.9	114.6	5.21	0.12
26.7	26.6	1.0	125.2	5.62	0.10
38.6	21.7	0.5	134.6	5.92	0.09
44.0	19.6	0.5	143.9	5.93	0.10
49.3	17.1	0.4	153.1	6.51	0.10
54.6	16.3	0.3	162.2	7.40	0.17
65.2	11.0	0.2	166.8	7.04	0.17
75.6	7.19	0.14	173.1	7.76	0.15

TABLE V—*Continued.*

θ	$\sigma(\theta)$	$\Delta_a\sigma$	θ	$\sigma(\theta)$	$\Delta_a\sigma$
		Run 13, $T_i=18.9$ Mev			
26.7	26.8	1.1	105.9	5.23	0.13
40.8	21.4	0.6	115.6	5.23	0.20
49.3	19.1	0.7	125.2	5.70	0.16
54.7	16.6	0.6	134.6	5.85	0.22
59.9	14.4	0.4	139.3	5.91	0.31
65.2	11.5	0.3	144.0	6.53	0.28
70.4	9.51	0.21	148.6	6.73	0.31
75.6	7.75	0.23	153.2	6.95	0.36
85.9	5.19	0.13	162.3	7.20	0.23
96.0	4.61	0.14	166.8	7.43	0.23
			171.3	7.33	0.32
		Run 14, $T_i=19.4$ Mev			
26.6	26.4	1.0	105.8	4.46	0.13
39.6	21.1	0.7	115.6	4.96	0.13
43.9	19.5	0.6	125.2	5.90	0.21
54.6	15.3	0.3	134.6	5.95	0.21
65.2	11.2	0.3	143.9	6.85	0.23
75.6	7.48	0.16	153.1	6.85	0.19
85.8	5.13	0.20	162.3	7.33	0.19
95.9	4.53	0.12	171.4	6.62	0.22

c. Protons on Carbon, $Q = -7.7$ Mev

Figure 6 shows the three distributions obtained for the 7.7-Mev excitation energy. Note the smallness of this cross section at its minima. A striking rapidity of variation with angle and energy is apparent except at small angles. This constancy with energy of the strong forward maximum suggests a direct-interaction process, though the behavior at larger angles is not in accord with the results so far obtained with this scattering model. (See Sec. 6b.)
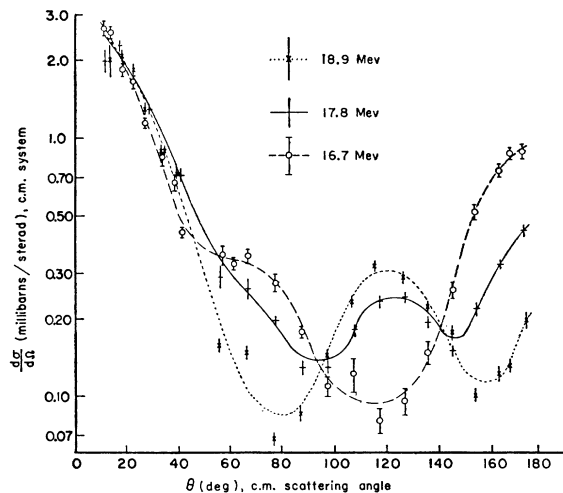
FIG. 6. $C^{12}(p,p')C^{12*}$, $Q=-7.7$ Mev. A plot of all data on the cross sections for inelastic scattering of protons from C^{12} leading to the excitation of the 7.7-Mev level. The curves are drawn primarily to connect the points measured at a given incident proton laboratory energy. Representative associated standard deviations are shown when larger than the points. Note the extent of the forward maximum of each distribution and the failure of the shape to remain reasonably constant.

d. Protons on Carbon, $Q = -9.6$ Mev

The angular distributions shown in Fig. 7 result from the excitation of the 9.6-Mev level of C^{12}. The small variation of the magnitude and shape of the cross sections as a function of energy hints that some sort of direct interaction is responsible for the scattering. Because of the difficulties here encountered at wide angles and low energies, no firm conclusion can be reached concerning the exact invariance of the angular distribution.

TABLE VI. Differential cross sections for excitation of the 7.7-Mev level of C^{12} by proton inelastic scattering. See Table II for notation and Table III for relevant experimental parameters. Repeated measurements are represented by weighted averages.

θ	$\sigma(\theta)$	$\Delta_a\sigma$	θ	$\sigma(\theta)$	$\Delta_a\sigma$
		Run 7, $T_i=16.7$ Mev			
11.7	2.63	0.15	87.2	0.177	0.008
13.9	2.55	0.13	97.3	0.108	0.010
18.4	1.84	0.06	107.2	0.121	0.019
22.8	1.65	0.05	116.9	0.080	0.009
27.3	1.14	0.05	126.3	0.095	0.012
33.9	0.83	0.05	135.6	0.148	0.014
38.3	0.67	0.05	144.8	0.258	0.014
41.6	0.43	0.02	153.8	0.52	0.03
56.8	0.350	0.028	162.7	0.74	0.04
61.1	0.324	0.012	167.1	0.87	0.02
66.4	0.349	0.019	171.5	0.88	0.03
76.9	0.274	0.023			
		Run 9, $T_i=17.8$ Mev			
12.1	1.96	0.20	97.5	0.130	0.08
17.7	2.27	0.11	107.4	0.181	0.009
23.2	1.76	0.08	117.1	0.231	0.011
28.7	1.28	0.05	126.6	0.241	0.007
34.2	0.90	0.03	135.9	0.197	0.010
40.8	0.72	0.05	145.1	0.150	0.007
56.0	0.288	0.030	154.1	0.218	0.010
66.6	0.260	0.022	163.1	0.325	0.012
77.1	0.196	0.006	172.0	0.438	0.023
87.4	0.129	0.009			
		Run 12, $T_i=18.9$ Mev			
13.8	2.00	0.28	96.9	0.144	0.006
18.3	2.06	0.11	106.8	0.233	0.014
22.7	1.82	0.09	115.6	0.320	0.014
27.1	1.29	0.08	126.0	0.289	0.017
33.7	0.88	0.05	135.4	0.223	0.011
39.2	0.72	0.09	144.6	0.176	0.013
55.4	0.157	0.018	153.7	0.100	0.008
66.1	0.149	0.009	162.7	0.123	0.011
76.5	0.068	0.005	167.1	0.131	0.007
86.8	0.085	0.006	173.3	0.196	0.015

e. Proton Scattering on Hydrogen

Each angular distribution for scattering on carbon was accompanied by some measurements on p-p scattering. Only a failure to know the chemical composition of the scattering foils can produce errors in the scattering from carbon which do not appear in these results. Figure 8 shows a summary of the current knowledge[20]

[20] Points not measured by the author, by Yntema and White,[11] or by Rotblat,[9] were taken from the summary in B. Cork, Phys. Rev. **80**, 321 (1952).

TABLE VII. Differential cross sections for excitation of the 9.6-Mev level of C^{12} by proton inelastic scattering. See Table II for notation, and Table III for relevant experimental parameters. Repeated measurements are represented by weighted averages.

θ	$\sigma(\theta)$	$\Delta_a\sigma$	θ	$\sigma(\theta)$	$\Delta_a\sigma$
Run 7, $T_i=16.7$ Mev					
14.1	6.38	0.36	51.0	5.48	0.13
18.6	5.97	0.27	77.8	5.41	0.22
23.2	5.82	0.23	88.1	5.32	0.22
27.7	5.79	0.40	98.2	3.7	0.4
34.4	5.50	0.32	127.1	2.2	0.5
38.8	5.81	0.26	136.3	2.9	0.4
42.2	5.90	0.26	145.4	1.2	0.3
Run 9, $T_i=17.8$ Mev					
17.8	5.13	0.47	98.3	4.79	0.19
23.5	5.51	0.38	108.1	4.04	0.22
29.1	5.82	0.39	117.8	3.52	0.19
34.6	6.80	0.24	127.2	2.53	0.18
41.3	6.10	0.30	136.5	1.70	0.12
45.7	5.77	0.27	145.6	1.23	0.13
67.3	5.77	0.28	154.5	0.86	0.07
77.8	5.86	0.18	163.3	0.42	0.09
88.1	5.47	0.23	172.1	0.37	0.05
Run 12, $T_i=18.9$ Mev					
14.0	7.47	0.77	87.3	5.69	0.13
18.5	7.43	0.27	97.7	5.02	0.11
23.0	8.10	0.41	107.3	4.15	0.28
27.3	7.69	0.33	116.2	3.42	0.17
34.1	6.61	0.37	126.7	2.74	0.17
39.6	7.17	0.32	136.0	1.86	0.07
45.1	6.36	0.25	145.1	1.03	0.09
50.6	6.42	0.51	154.0	0.68	0.09
66.7	6.74	0.23	162.9	0.59	0.06
77.2	6.13	0.17	167.3	0.12	0.06

of the 90-deg c.m. p-p cross section as a function of energy. The good agreement of the author's measurements with the previously published values is taken as an indication of the accuracy of both. In placing the data from this experiment on the curve for 90-deg scattering, use was made of the very slight angular

TABLE VIII. Integrated partial cross sections as a function of energy for the excitation of the 4.4-, 7.7-, and 9.6-Mev levels of C^{12} by proton inelastic scattering. The integrals were obtained using a 10-deg net after extrapolation of the measurements to small and large angles. Cross sections are given in millibarns, along with the total combined estimated standard deviations. Note that a nuclear radius of 3.3×10^{-13} cm for carbon would indicate a "geometrical" reaction cross section of about 340 mb.

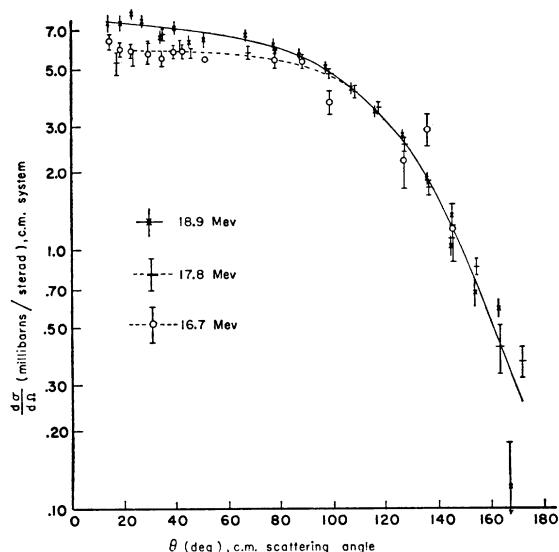| Run	T_i(Mev)	$-Q$ 4.4 Mev	7.7 Mev	9.6 Mev
1	14.0	225±8		
2	14.7	206±6		
3	15.2	210±7		
4	15.6	196±6		
5	16.2	179±5		
6	16.7	160±5		
7	16.7	154±4	4.8±0.2	51±2
8	17.4	137±6		
9	17.8	144±4	4.6±0.2	55±2
10	17.9	130±6		
11	18.4	124±6		
12, 13	18.9	127±3	4.2±0.2	60±2
14	19.4	127±4		

FIG. 7. $C^{12}(p,p')C^{12*}$, $Q=-9.6$ Mev. Differential cross sections for the inelastic scattering of protons from C^{12} with $Q=-9.6$ Mev. The curves are drawn primarily to connect the points measured at a given incident proton laboratory energy. Representative associated standard deviations are shown when larger than the points. Note the extent to which the shape is constant as a function of bombarding energy.

dependence of the p-p cross sections in the range between 40-deg c.m. and 90-deg c.m.

6. COMPARISON WITH THEORIES OF INELASTIC SCATTERING

The comparison of the inelastic scattering distributions with theory must be circumscribed by the knowl-
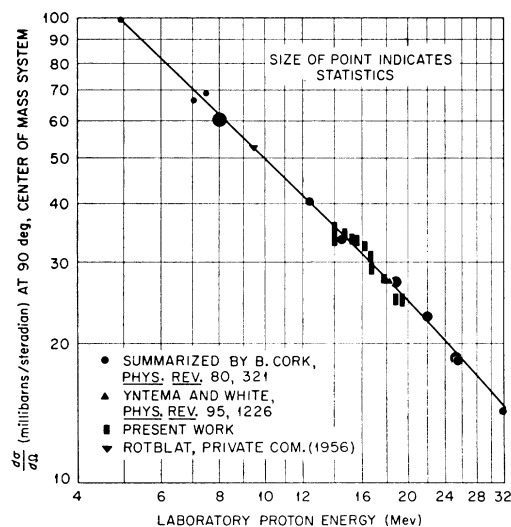

FIG. 8. A summary of data on the 90-deg c.m. scattering of medium-energy protons on hydrogen. The bars which represent the present work are averages of cross sections measured at angles between 40 and 90 deg c.m.; the height of each bar indicates total estimated standard deviation. The diameters of the points taken from Cork[20] indicate errors listed there. An arbitrary curve was fitted to the points by eye.
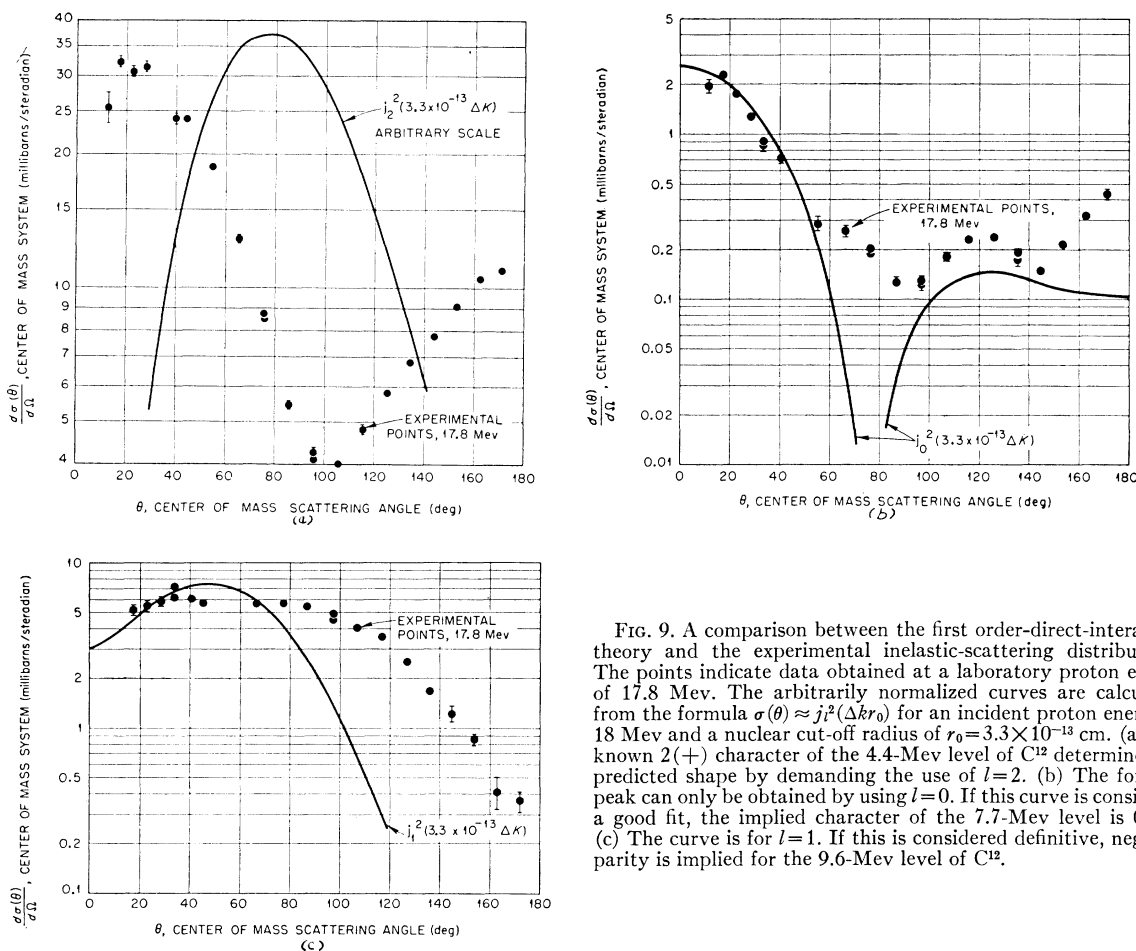
FIG. 9. A comparison between the first order-direct-interaction theory and the experimental inelastic-scattering distributions. The points indicate data obtained at a laboratory proton energy of 17.8 Mev. The arbitrarily normalized curves are calculated from the formula $\sigma(\theta) \approx j_l^2(\Delta k r_0)$ for an incident proton energy of 18 Mev and a nuclear cut-off radius of $r_0 = 3.3 \times 10^{-13}$ cm. (a) The known 2(+) character of the 4.4-Mev level of C^{12} determines the predicted shape by demanding the use of $l = 2$. (b) The forward peak can only be obtained by using $l = 0$. If this curve is considered a good fit, the implied character of the 7.7-Mev level is 0(+). (c) The curve is for $l = 1$. If this is considered definitive, negative parity is implied for the 9.6-Mev level of C^{12}.

edge that no current theoretical prediction is expected to be accurate in this region of energy and mass number. A compound-nucleus theory[21,22] and the first-order direct-interaction theory[23,24] are discussed below as limiting cases for which calculations have been made. The predictions of these models are discussed with relation to the current experiment. Thomas[25] has already pointed to a conceptual and scattering-theoretical method for integrating into a single scheme the ideas behind these two limiting cases.

a. Compound Nucleus Theory

The papers of Wolfenstein[21] and of Hauser and Feshbach[22] derive the angular distributions to be expected in the case of neutron inelastic scattering leading through an effective continuum of compound states to a discrete final state in the residual nucleus. These derivations specifically require a statistical assembly of

every relevant compound-nucleus level character to be present within the beam energy spread. The most easily checked prediction of this theory is that the inelastic scattering should have symmetry about 90 deg. The failure of this prediction in the present case can be explained by the inappropriateness of the statistical assumption, for Vogt[26] estimates a level spacing of about 0.6 Mev for levels of a given character in the N^{13} compound nucleus. Failure of the statistical assumption alone, however, cannot explain the consistent forwardness of the scattering.

b. Direct Interaction Theory

The case of the (n,p) reaction in the intermediate energy region has twice been calculated[23,24] in the approximation of a direct two-body interaction between the incident and effluent particles. This interaction is supposed to take place on the fringe of the nuclear potential. Angular distributions are obtained which take the form

$$\sigma(\theta) \approx j_l^2(\Delta k r_0),$$

[21] L. Wolfenstein, Phys. Rev. **82**, 690 (1951).
[22] W. Hauser and H. Feshbach, Phys. Rev. **87**, 366 (1952).
[23] N. Austern *et al.*, Phys. Rev. **92**, 350 (1953).
[24] M. Demeur, J. phys. radium **16**, 73 (1955).
[25] R. G. Thomas, Phys. Rev. **100**, 25 (1955).

[26] Erich Vogt (private communication, 1954).

where j_l is the lth order spherical Bessel function, r_0 is the minimum radius at which the interaction is supposed to be important, and Δk is the momentum transfer to the nucleus. The predicted variation with angle thus depends on the energetics of the reaction and the chosen cut-off radius, but in general there should be forward peaks which change smoothly with energy and atomic weight. The most general of the selection rules governing l is that

$$|\mathbf{J}_0| + |\mathbf{J}_n| + 1 \geq l \geq |\mathbf{J}_0 + \mathbf{J}_n + \mathbf{S}|_{\min}.$$

$\mathbf{J}_0$ and $\mathbf{J}_n$ are the total vector spins of the target and residual nuclei. $\mathbf{S}$ is a unit vector unless $\mathbf{J}_0 = \mathbf{J}_n = 0$, in which case $\mathbf{S} = 0$. Conservation of parity requires that l be odd or even according to whether or not there is a difference of parity between the states of the target and residual nuclei.

Before the results of this experiment are compared with the predictions of the theory just described, it should be noted that the calculations were carried out in the Born approximation for the (n,p) reaction, that no details of the nuclear wave function have been included, and that the simple angular dependence is only supposed to be reasonably accurate in the extreme forward direction even under the assumptions made. An attempt to remove some of these difficulties has been reported by Banerjee, et al.[27] for the cases of Li[6] and C[12].

Figure 9 (top) presents a strong contrast between the experiment and the predicted simple Bessel-function distribution for the excitation of the 4.4-Mev level. The spin and parity of the ground and first excited states of C[12] are presumably known to be 0(+) and 2(+), so one is not free to vary the value of l.

The comparison in Fig. 9 (middle) for the excitation of the 7.7-Mev state of C[12] is more encouraging. The data are fitted with a curve calculated for $l=0$, the only possibility in this simple theory for the strong forward peak. This choice is consistent with suggestions[28] in the literature that the 7.7-Mev level is a 0(+) state. The behavior of the experimental cross sections at larger angles appears anomalous from this first order direct-interaction viewpoint.

Figure 9 (bottom) compares a distribution measured for the 9.6-Mev level with the direct interaction theory Bessel-function distribution calculated for $l=1$. The degree of agreement shown is much better than that which can be obtained with $l=0$ or $l=2$. Should this

comparison be considered a fit, odd parity would be indicated for the 9.6-Mev level. While the behavior with energy of this angular distribution is seen to favor a non-compound-nucleus interaction, a statement that the indicated degree of fit implies a negative parity for the level would be premature. A negative parity level is impossible within the p^8 shell configuration which is usually used to predict[29,30] energy level structure of C[12] in this region of excitation energy.

Difficulty is experienced in discerning the physical meaning of the evidences of fit in the above comparisons because there is no knowledge of the degree of uniqueness of the assumptions which in low approximation give rise to the simple Bessel-function distributions. This problem can be settled only by further theoretical inquiry.

7. SUMMARY OF CONCLUSIONS

The elastic scattering distributions are doubtless close to being understood by means of the complex-potential model, but the possibility seems remote that the parameters might change with energy in a simple manner. The first strong impression of the inelastic data must be the large variation between the shapes of the distributions corresponding to the various levels of C[12]. No currently popular model has led to calculated distributions which explain even the qualitative features. No evidence is found here for the type of distribution predicted by the compound-nucleus theory with statistical assumptions, but the conditions of this theory are not well met. The comparison of the data with the direct-interaction theory is more positive, but no clear-cut verification of the simple distributions calculated for (n,p) reactions has been found in these results.

ACKNOWLEDGMENTS

[27] Banerjee, et al., Bull. Am. Phys. Soc. Ser. II, 1, 194 (1956).
[28] G. Harries, Proc. Phys. Soc. (London) A67, 153 (1954).
[29] D. R. Inglis, Revs. Modern Phys. 25, 390 (1953).
[30] D. Kurath, Phys. Rev. 101, 216 (1956).